ELSEVIER

Coordination Chemistry Reviews
219–221 (2001) 1055–1074

COORDINATION CHEMISTRY REVIEWS

www.elsevier.com/locate/ccr

Structural mimics for the active site of [NiFe] hydrogenase

Andrew C. Marr, Douglas J.E. Spencer, Martin Schröder *

School of Chemistry, University of Nottingham, University Park, Nottingham NG7 2RD, UK

Received 13 December 2000; accepted 25 May 2001

Contents

Abstract

Hydrogenases are enzymes that catalyse the reversible two-electron oxidation of H_2. The [NiFe] hydrogenases have been characterised spectroscopically and by single crystal X-ray diffraction, and show an active site incorporating a heterobinuclear [NiFe] centre bridged by two cysteine S-donors. Low molecular weight synthetic complex models, which structurally mimic the dithiolate-bridged [NiFe] centre, serve as important probes of structure and

* Corresponding author. Tel.: +44-115-951-3490; fax: +44-115-951-3563.
E-mail address: m.schroder@nottingham.ac.uk (M. Schröder).

PII: S0010-8545(01)00396-4

chemistry at the active site and are the subject of this review.

Keywords: [NiFe] Hydrogenase; Modelling; Nickel; Iron; Thiolate; Synthesis; Bioinorganic

1. Introduction

Hydrogenase enzymes catalyse the reversible two-electron oxidation of H_2 in aerobic and anaerobic micro-organisms [1]. They can either oxidize H_2 to H^+ or reduce H^+ to H_2 and therefore provide a reversible sink for multi-electron transfer. Hydrogenases play a major role in the fermentation of biological substances to CH_4 and in microbial phosphorylation, where H_2 can either serve as an energy source in place of NADH or be generated as the product of reductive processes [2].

$$H_2 \rightleftharpoons 2H^+ + 2e^-$$

The reversible oxidation of H_2 provides electrons at a low potential ($H_2/2H^+$: $E^0 = -414$ mV at pH 7 and 1 atm of H_2 vs. NHE) [3], but H_2 activation is energetically unfavourable due to the low acidity of the H–H bond ($pK_a = 35$). Binding to a metal centre can decrease this energetic barrier by between 20 and 30 units [4,5], thus facilitating the heterolytic cleavage of H_2 to give H^+ and H^-, a potential first step in the oxidation process.

Metal-containing hydrogenases can be divided into three groups, [NiFe] hydrogenases, [NiFeSe] hydrogenases and [Fe]-only hydrogenases. The [NiFe] hydrogenases and [NiFeSe] hydrogenases contain a heterodinuclear active site while [Fe]-only hydrogenases contain a homodinuclear active site [6–8]. The majority of hydrogenases contain Fe–S clusters, which are arranged to facilitate electron transfer to and from the active site [9,10]. The [NiFeSe] hydrogenases also contain one equivalent of Se per Ni in the form of selenocysteine ligated to the Ni centre [10–16]. As well as catalysing the reversible oxidation of H_2, [NiFe] hydrogenase has exhibited the ability to catalyse proton–deuterium and proton–tritium exchanges in the absence of electron-donors or acceptors, for example, H^+/D_2 exchange in water [17].

$$H_2O + D_2 \rightleftharpoons HDO + HD$$

2. [NiFe] Hydrogenase

2.1. Structure

Examples of [NiFe] hydrogenases that have been studied extensively include the hydrogenases from the photosynthetic bacteria *Chromatium vinosum* and *Thiocapsa roseopersicina* [18–22] (*C. vinosum* and *T. roseopersicina*, respectively) and *Desulfovibrio gigas* (*D. gigas*) from the sulphate-reducing bacteria belonging to the *Desulfovibrio* genus [1]. The structure of [NiFe] hydrogenase from *D. gigas* has been

determined by X-ray crystallography to a resolution of 2.85 and 2.54 Å [1,23]. As isolated, in an oxidised and inactive form, the enzyme is a heterodimeric periplasmic protein consisting of two subunits, one large (60 kDa) and one small (28 kDa). The protein contains a total of 12 atoms of Fe, 12 acid labile sulphides and one atom of Ni [24–26]. Eleven of the twelve Fe atoms are incorporated within three Fe–S clusters, one $[3Fe–4S]^{1+/0}$ and two $[4Fe–4S]^{2+/+}$ moieties which lie almost linearly in the small sub-unit ca. 12 Å apart (Fig. 1). The $[3Fe–4S]^{1+/0}$ cluster is situated approximately half-way between the two $[4Fe–4S]^{2+/+}$ clusters; one $[4Fe–4S]^{2+/+}$ cluster, the proximal or p-cluster, is 13 Å from the active site and the other, the distal or d-cluster, lies close to the surface of the metalloenzyme. The remaining Fe centre resides with Ni at the active site of the enzyme, which is buried deep inside the large sub-unit. The linearity of the Fe–S clusters implies that they are part of an electron-pathway between the active centre and the molecular surface. The oxidation of H_2 is a two-electron process each electron being transferred separately to the outlying $[4Fe–4S]^{2+/+}$ distal cluster and subsequently passed on to cytochrome c_3, the hydrogenase 'redox partner'. It is postulated that the second electron remains at the active site until the $[4Fe–4S]^{2+/+}$ cluster is reoxidised [27].

The active site (Fig. 2) comprises a heterobimetallic [NiFe] centre [1,23,27,28]. The Ni centre is ligated by four cysteinates, two of which are terminal and two that bridge to Fe. The Fe centre is ligated further by three non-protein diatomic ligands, with a third bridging ligand completing the active site; this additional bridging species has been assigned as oxo oxygen more closely associated to Ni than Fe [10].

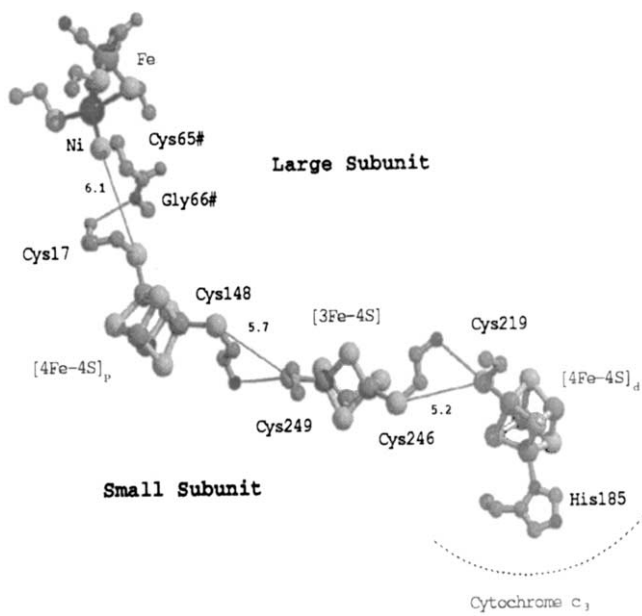

Fig. 1. The metal containing sub-units of [Ni–Fe] hydrogenase [1,3,27,31].

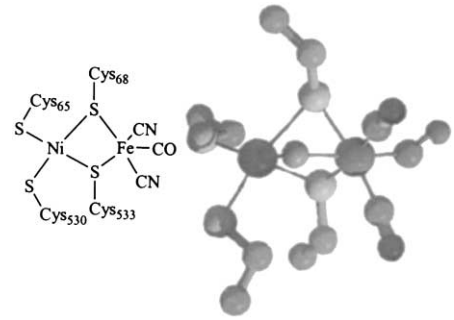

Fig. 2. The heterobimetallic active site in [Ni–Fe] hydrogenase [1,3,27,31].

Ni lies in a distorted square pyramidal geometry with the bridging cysteinate Cys533 occupying the position above the plane. Fe is in a distorted octahedral low-spin environment. The Fe–S–Ni angle is acute and this brings the metals within close proximity, resulting in a Ni–Fe distance of 2.9 Å. Activation of the enzyme is believed to involve loss of the oxo ligand and contraction of the Ni–Fe distance to some 2.5–2.6 Å [22]. Infrared (IR) spectroscopic studies have led to the assignment of the three diatomics co-ordinated to Fe as two CN^- and one CO ligand [18,19,23,28], with the CN^- ligands hydrogen-bonding with the protein and the CO ligand lying in a hydrophobic pocket.

Recently, a crystal structure of [NiFe] hydrogenase from *D. desulfuricans*, which contains one SO and a mixture of CN^- and CO ligands on Fe, has been reported [29]. Although related this is however not typical of other structures reported for [NiFe] hydrogenases and will not be discussed further within this review.

2.2. Redox chemistry and catalytic mechanism

For extensive reviews of the redox and spectroscopic properties of [NiFe] hydrogenases the reader is directed towards the reviews by Halcrow et al. [30], Fontecilla-Camps and Ragsdale [10], Fontecilla-Camps [31] and Frey [27]. This section is intended as an introduction.

The redox chemistry of [NiFe] hydrogenase is complex as Ni, Fe and cysteinates are all capable of different oxidation states [10]. The EPR spectroscopic studies have been used as the primary tool for distinguishing between the different redox states of the enzyme and these will form the basis for this discussion [17,32–41]. The redox forms of the enzymes discussed are summarised in Fig. 3. It is noteworthy that the separation between the most oxidised and reduced forms of the enzyme is only ca. 300 mV.

[NiFe] Hydrogenase from *D. gigas* is isolated in the oxidised form, which is not catalytically active. The oxidised form of [NiFe] hydrogenase contains two EPR active forms Ni-A and Ni-B which exhibit rhombic spectra with g values of 2.32, 2.23, 2.01 and 2.34, 2.16 and 2.01, respectively. It is generally accepted that both forms contain Ni(III), low-spin Fe(II) ions and bound oxygen [37]. Ni-A and Ni-B

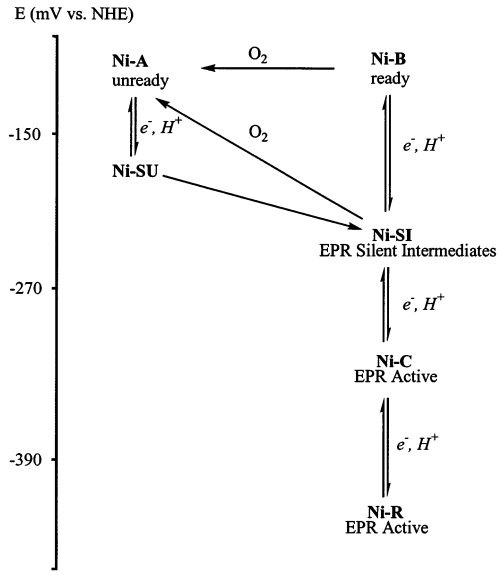

Fig. 3. The redox states of [NiFe] hydrogenase [10].

are both reduced and activated in the presence of H_2 but their reactivities differ. Ni-A is termed the 'unready state' as activation is slow and temperature dependent. Reduction by one-electron generates an EPR-silent, catalytically inactive form labelled Ni-SU ('nickel-silent and unready'). The Ni-B state is termed 'ready' as it is reduced rapidly to one or more active species in the presence of H_2 and low potential electron-acceptors [37]. Partial activation (one-electron reduction) of Ni-B yields an EPR-silent intermediate, termed Ni-SI [32], which actually represents two forms distinguishable by IR spectroscopy [23,28]. Anaerobic oxidation of Ni-SI with $[Fe(CN)_6]^{3-}$ regenerates Ni-B exclusively, while incubation with O_2 gives a mixture of Ni-A and Ni-B. If Ni-B is fully activated via a two-electron reduction, or if Ni-SI undergoes further activation via a one-electron reduction, a new EPR active state termed Ni-C is observed. The Ni-C state is thermally stable in the absence of H_2 and cannot spontaneously reduce protons to H_2 [32], but it is photosensitive [40]. Ni-C exhibits a rhombic EPR spectrum with g values of 2.19, 2.16, 2.01 [17,35–39]. Further reduction of the Ni-C state by one-electron with H_2 forms a fully reduced state termed Ni-R, which is EPR-silent and unstable in the absence of H_2. The spectrum for Ni-C can be regenerated directly from Ni-R.

There have been many attempts to rationalise the spectra and assign structures and oxidation states to the observed species, but this has proven difficult due to the complexity of the system. For an in-depth discussion of the latest theories the reader is directed to the recent reviews by Fontecilla-Camps and Ragsdale [10], Fontecilla-Camps [31] and Frey [27]. Attention has been focussed most upon the Ni centre as many believe that Ni is the site of hydride binding [4], and there has been much discussion concerning the form(s) of the enzyme that act as the H_2 oxidant in

the catalytic cycle. Ni-C and Ni-SI have emerged as the most likely candidates [42,43]. Ni-C has attracted great attention, as it appears to be the only EPR-active state, which participates, in the catalytic activity [10]. Several hypotheses have been proposed concerning the nature of Ni-C as Ni(I) or Ni(III) with unbound H_2 or bound H_2, H^+ and H^- [22,32,38,44–50].

Maroney et al. have carried out extensive work concerned with assigning the redox states of the enzyme [22,33]. After initial studies, they postulated a redox-active ligand-based mechanism [33]. In this model, the EPR signal for Ni-C is generated by a thiyl radical and a Ni(II) ion; significantly, this is isoelectronic with a thiolate bound Ni(III). Dole et al. [51] and Fontecilla-Camps and Ragsdale [10] have also postulated mechanisms based on ligand-based redox chemistry. More recently, Maroney et al. have studied [NiFe] hydrogenase from *Chromatium vinosum* by X-ray absorption and revised their model [22a]. From analysis of nickel K-edge energy shifts they concluded that activation of the enzyme involves a change in electron density on nickel consistent with the reduction of Ni(III) to Ni(II). They were able to assign EPR-active states Ni-A, Ni-B and Ni-C to Ni(III) and the EPR-silent states to Ni(II). Furthermore, XANES enabled them to assign the geometry of Ni-A, Ni-B and Ni-SU forms as the five co-ordinate species, and Ni-SI and Ni-R forms as the four co-ordinate distorted planar species. In contrast, Ni-C may actually involve six coordination at Ni. These workers also reported that conversion from the Ni-B to the Ni-SI form is accompanied by a contraction in the Fe–Ni distance from 2.9 to 2.5–2.6 Å. Their assignments are summarised in Fig. 4. Barondeau et al. [42] have implicated Ni-SI as the active oxidant and Ni-R as the active reductant in the cycle. The debate on the role of the Ni centre in this system continues, and modelling both by synthesis and calculation continues to contribute to the theories proposed.

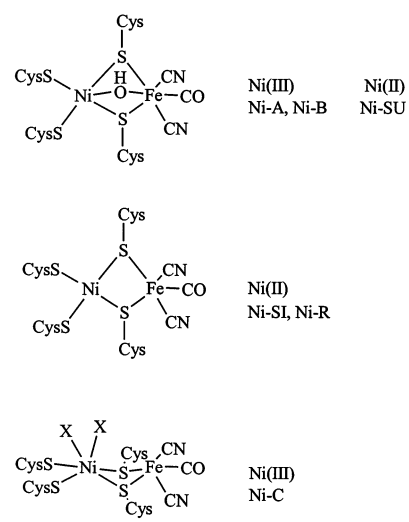

Fig. 4. Proposed structure of redox forms of [NiFe] hydrogenase [22a].

The role of Fe is also unclear. Volbeda et al. have observed slight frequency shifts in the IR spectrum as a function of the redox state of the enzyme, indicating that the Fe centre may be 'non-innocent' in the redox process [23,28] (Table 1). The role of the cysteinates is also still under discussion and the extent of their 'non-innocent' behaviour within the catalytic cycle is still not clear, although mechanisms have been proposed involving them as reactive entities in the cycle [10,22,51]. Cysteinate may participate in the activity of the enzyme as a Brønsted base; indeed, the concerted action of a Lewis-acid metal and basic cysteinate may facilitate the heterolytic cleavage of H_2 to form a metal hydride and co-ordinated cysteine (Fig. 5) [1,23,52–55]. Functional models have shown that the base-assisted heterolytic cleavage of H_2 gives rise to metal hydrides [54–56]; this has been particularly well illustrated for a four co-ordinate Ni(II) complex by Sellmann et al. [54], while Roberts and Lindahl [45] have suggested that protonated cysteinates are involved in the redox chemistry of the enzyme. Gessner and co-workers [20,21] have reported orientation-selected ENDOR studies on *C. vinosum* and single crystal EPR spectra of *D. gigas* in the oxidised or 'ready' state and their findings are consistent with 'non-innocent' cysteine residues. The ENDOR studies exhibited three distinct protons for the Ni-B state: two were assigned to the β-methylene protons from the bridging Cys533 residue, the observed large coupling being derived from substantial spin-delocalisation onto the bridging Cys533 residue. The third proton was assigned to a β-methylene proton of the Cys68 residue or a protonated Cys65 or 530 residues. These observations were corroborated by single crystal experiments.

The catalytic mechanism of the enzyme is still far from clear and hypotheses are constantly being proposed and modified as new data are reported. It is certainly remarkable that a two-electron process can be catalysed by an active site, which exhibits redox processes within such a narrow potential (-100 to -400 mV vs. NHE at pH 7) [1,23,52,53]. It is clear from the shift in the IR frequencies of the

Table 1
Changes in ν_{CO} and ν_{CN} as a function of redox state [23,28]

Redox state	ν_{CO} (cm^{-1})	ν_{CN} (cm^{-1})	ν_{CN} (cm^{-1})
Ni-A	1947	2083	2093
Ni-B	1946	2079	2090
Ni-SI_I	1914	2055	2069
Ni-SI_{II}	1934	2075	2086
Ni-C	1952	2073	2086
Ni-R	1940	2060	2073

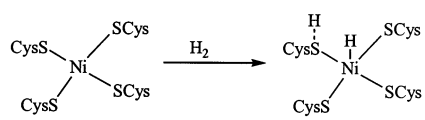

Fig. 5. Proposed mechanism of heterolytic cleavage of H_2.

diatomic ligands as a function of the redox state of the enzyme (Table 1), [23,28] that the changes in redox state are sensed by both metal centres [23]. It would therefore appear to be prudent to consider the Ni-dithiolate-Fe moiety as a whole rather than separate, non-interacting units.

The redox chemistry of [NiFe] hydrogenase is further complicated by the presence of two [4Fe–4S] clusters that have mid-point redox potentials (ca. -290 and -340 mV vs. NHE at pH 7) [57–59] similar to those observed for the Ni-SI/Ni-C (-380 mV) and Ni-C/Ni-R (-445 mV) [23]. Therefore, any overall description of the states of hydrogenase must be inclusive of these clusters. Interestingly, the [3Fe–4S] cluster has a significantly more anodic mid-point potential, ca. -30 to -80 mV, [35,57,60] raising the question of whether this cluster actually participates in the electron-transfer process.

This review is primarily concerned with attempts to understand the relationship between the structure and activity of the active site of [NiFe] hydrogenase. Many questions about the nature and function of the active site remain unanswered. Why is the Ni centre surrounded entirely by thiolates? Why are three non-protein diatomic ligands co-ordinated to the Fe centre? Why are there two metals at the active site? Why is the Fe centre low-spin? Synthesis and theory have been directed at the structure–function relationship in this important class of metalloenzymes and their small molecule mimics.

2.3. Theoretical and computational modelling of the active site

The results of theoretical and computational modelling have suggested a variety of possibilities relating to the mechanism of H_2 oxidation, and generally these models point to a degree of participation of the ligand in the catalytic process. Gioia et al. [61] used density functional theory to model the structure of [NiFe] hydrogenases. Their calculations suggested that the Fe remains in the same valence state throughout the catalytic cycle and that the redox processes are a property of the cluster as a whole, including the cysteinate moieties. Fontecilla-Camps and co-workers [62] have recently carried out a hybrid density functional theory on the [NiFe] hydrogenase active site redox states, which agrees with the findings of Gioia et al. [61]. They suggested that Cys530 is a 'non innocent' ligand and may act as a base in the catalytic cycle. They also concluded that Fe(II) is *not* redox active and remains in the $+2$ oxidation state throughout, and that the redox chemistry is centred at the Ni ion, the cysteinates and the hydrogen species. They ruled out the involvement of thiyl radicals. In contrast, Niu et al. [63] have proposed that the site of H_2 binding is at the Fe centre, and suggested that the geometric constrictions imposed at the active site by the surrounding protein play a vital role in H_2 activation with involvement of the cysteinates again proposed.

In terms of co-ordination chemistry, the active site of [NiFe] hydrogenase in *D. gigas* is unique and many workers have struggled to prepare structural models with functional complex modelling being a longer term goal. Recreating the important structural features of the active site within low molecular weight analogues allows the testing and modelling of the reactivity and redox properties in

order to recognise the features of the active site which are vital to enzyme activity. As a heterobimetallic thiolate bridged species containing diatomic ligands [NiFe] hydrogenase has a unique structure, and represents an exciting challenge for the synthetic chemist. The remainder of this review describes the attempts to reproduce the structural features observed at the active site of [NiFe] hydrogenase.

3. Structural models of [NiFe] hydrogenase

Until the structural elucidation of the active site of [NiFe] hydrogenase from *D. gigas* by Volbeda and co-workers [1,23,28] in 1996, it was accepted widely that a thiolate-ligated mononuclear or binuclear Ni centre was present [30]. As a result, much of the early work concentrated on compounds incorporating mononuclear and binuclear Ni centres ligated by thiolates, thioethers and amines [33,64–71]. This work provides the foundations for the current work on mixed [NiFe] thiolate-bridged centres. The work incorporating binuclear and mononuclear Ni complexes can be found in recent reviews by Fontecilla-Camps and co-workers [10,52] and will not be discussed further here. This review will focus specifically on heterodinuclear [NiFe] complexes bridged by thiolate ligands.

3.1. Monometallic thiolate precursors

An important synthetic route to thiolate-bridged heterobimetallic complexes is the addition of a solution of a metal complex with labile ligands to a mononuclear metal thiolate complex. A major synthetic difficulty arises from the high tendency of metal thiolate complexes to aggregate to form a variety of homometallic clusters [72]. The chemoselectivity of the cluster-forming step is also difficult to control and mixed-metal clusters are likely reaction products [73]. The most successful method of controlling the chemistry of the mononuclear thiolate precursor has been to incorporate the thiolates within a polychelate ligand, which wraps around the metal centre. This employs the chelate effect to prevent dissociation of the thiolate-containing ligand and directs subsequent reactions with metal salt and complex reagents towards the terminal thiolate donors (Fig. 6).

3.1.1. Nickel thiolate precursors

The most common methodology to mixed NiFe complexes has been via reaction of a Ni(II) thiolate complex with a labile Fe species. This method has been employed to prepare a range of synthetic models.

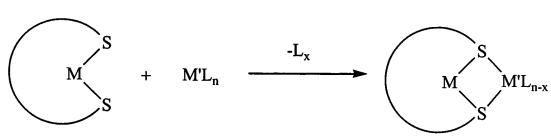

Fig. 6. Preparation of Ni–Fe unit via a monometallic thiolate precursor.

Pohl and co-workers reported [74] the reaction of the Ni(II) thiolate species [Ni(L)] [L = *N*,*N*′-diethyl-*N*,*N*′-bis(2-mercaptoethyl)-1,3-propanediamine] with the tetraiodo cluster anion $[Fe_4S_4I_4]^{2-}$ to yield $[Ni(L)(Fe_4S_4I_2)(L)Ni]$ (Fig. 7). The cluster $[Ni(L)(Fe_4S_4I_2)(L)Ni]$ incorporates a dithiolate bridge between Ni and Fe centres with a Ni–Fe distance of 2.827(1) Å. $[Ni(L)(Fe_4S_4I_2)(L)Ni]$ exhibits a quasi-reversible oxidation wave at $E_{1/2} = +0.15$ V (vs. SCE) which lies between that observed for $[Fe_4S_4(S'Bu)_4]^{2-}$ ($E_{1/2} = -0.11$ V vs. SCE) [75] and $[Fe_4S_4I_4]^{2-}$ ($E_{1/2} = +0.55$ V vs. SCE) [76]. The corresponding monosubstituted cluster anion $[Ni(L)Fe_4S_4I_3]^{-}$ was also reported (Fig. 8) [74].

Bouwman et al. have reported [73] the reaction of [Ni(dsdm)] [H_2dsdm = *N*,*N*′-dimethyl-*N*,*N*′-bis(2-sulfanyl-ethyl)ethylenediamine)] with $K[HFe(CO)_4]$ to give, via reshuffling of the ligands and of the metal oxidation states, $[Fe(dsdm)Ni(CO)_3]_2$ (Fig. 9). The reported structure consists of a Ni(0)–Fe(II)–Fe(II)–Ni(0) core, with one thiolate from each dsdm ligand bridging the two Fe(II) centres, and the remaining thiolates bridging Fe(II) and $Ni(CO)_3$ moieties. The Fe(II) and the Ni(0) ions are in trigonal bipyramidal and tetrahedral geometries, respectively, and the Ni–Fe distance is relatively long at 3.899(1) Å. No electrochemical data were reported for the complex.

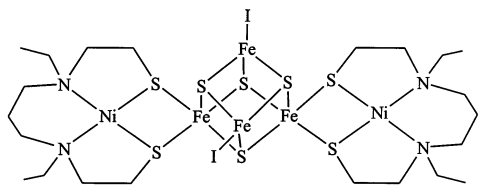

Fig. 7. The structure of $[Ni(L)(Fe_4S_4I_2)(L)Ni]$ [74].

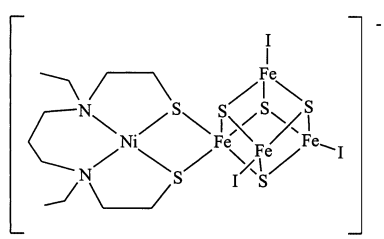

Fig. 8. The structure of $[Ni(L)Fe_4S_4I_3]^{-}$ [74].

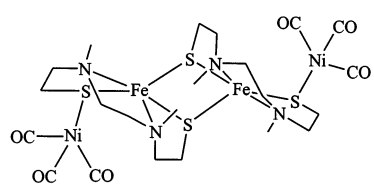

Fig. 9. The structure of $[Fe(dsdm)Ni(CO)_3]_2$ [73].

[Ni(L)] [L = *N*,*N*′-dimethyl-*N*,*N*′-bis(2-mercaptoethyl)-1,3-propanediamine] has been utilised by Maroney and co-workers as a precursor to Ni–Fe compounds [70,71]. Thus, reaction of [Ni(L)] with $[Fe(H_2O)_6](ClO_4)_2$ gave $[\{Ni(dmpn)\}_3Fe](ClO_4)_2$ (Fig. 10), the single crystal X-ray structure of which confirms the formation of a Ni_3Fe cluster with mono- and di-thiolato bridges. The cluster contains a central high-spin Fe(II) surrounded by five thiolate donors, which form bridges to three square-planar Ni(II) centres. The sixth thiolate is at a non-bonding distance of 3.197(8) Å, while the Ni(II) centres have near perfect square-planar arrangements, similar to the mononuclear precursor [Ni(L)] moieties. The Ni–Fe distances in $[\{Ni(dmpn)\}_3Fe](ClO_4)_2$ are 2.976(4), 3.123(3) and 3.269(4) Å.

Pohl and co-workers have reported [77] a Ni–Fe complex derived from [Ni(L)] [L = *N*,*N*′-dimethyl-*N*,*N*′-bis(2-mercaptoethyl)-1,3-propanediamine]. Thus, reaction of [Ni(L)] with $[Fe(CO)_2(NO)_2]$ yields $[Ni(L)Fe(NO)_2]$ (Fig. 11), which shows the Ni(II) ion in a square-planar N_2S_2 environment with the Fe centre in a distorted tetrahedral co-ordination environment ligated by two bridging thiolates and two terminal NO ligands. As the NO groups are bound in a linear fashion, they may be regarded as formally $3e^-$ donors. The oxidation state at Fe can therefore be assigned as -2 with the complex having an overall 18-electron configuration. The Ni–Fe distance is relatively short at 2.797(1) Å with the ∠Ni–S–Fe angles somewhat acute at 76.11(4) ° similar to the angles of 74 ° observed in the active site [23]. Electrochemical studies on $[Ni(L)Fe(NO)_2]$ confirm that the complex exhibits a quasi-reversible oxidation at $E_{1/2} = -0.12$ V (vs. SCE) assigned to the Fe$(-2/-)$ couple on the basis that oxidation of [Ni(L)] does not occur below $+0.86$ V (vs. SCE). Chemical oxidation of $[Ni(L)Fe(NO)_2]$ led to decomposition with no pure products isolated.

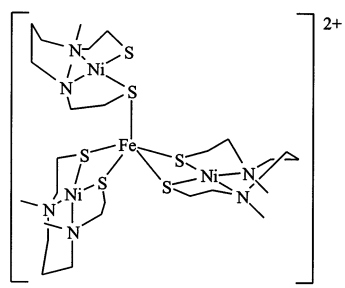

Fig. 10. The structure of $[\{Ni(dmpn)\}_3Fe](ClO_4)_2$ [70,71].

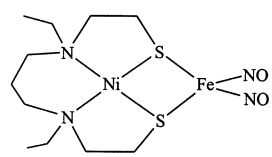

Fig. 11. The structure of $[Ni(L)Fe(NO)_2]$ [77].

Darensbourg and co-workers have reported [78–80] a number of structures incorporating thiolate bridged Ni–Fe centres prepared from monometallic nickel thiolate precursors. Thus, reaction of (H_2L) [L = *N*,*N*′-bis(2-mercaptoethyl)-1,5-diazacyclooctane] with Ni(II) yields [Ni(L)] which reacts further with anhydrous $FeCl_2$ to form [Ni(L)FeCl(μ-Cl_2)ClFe(L)Ni] (Fig. 12) [80]. The Ni(II) and Fe(II) ions in this complex have square-planar and pseudo-square-pyramidal geometries, respectively, and lie 3.100(1) Å apart. The thiolate donors and the bridging Cl^- provide the basal plane to the square pyramid at Fe(II), with the terminal Cl^- occupying the axial site to give a planar Fe_2(μ-Cl)$_2$ core. [Ni(L)FeCl(μ-Cl_2)ClFe(L)Ni] shows a reversible reduction at $E_{1/2} = -0.64$ V assigned to a Ni(II)/Ni(I) couple, and an irreversible reduction at $E_{pc} = -1.53$ V (vs. NHE). Darensbourg and co-workers have also reported the reaction of [Ni(L)] [L = *N*,*N*′-bis(2-mercaptoethyl)-1,5-diazacyclooctane] with [$Fe_2(CO)_9$] to form [Ni(L)Fe(CO)$_4$] (Fig. 13) [79] in which the Ni and Fe centres remain in their original oxidation states of +2 and 0, respectively. The Fe(CO)$_4$ fragment is bound to [Ni(L)] via a single thiolate bridge which occupies an axial position at Fe(0) and the Ni–Fe distance of 3.76(1) Å is too long for any potential interaction. The Fe(0) centre has a slightly distorted trigonal bipyramidal geometry, while the Ni(II) centre remains essentially planar. [Ni(L)Fe(CO)$_4$] was an early example of bridging between Ni and a single Fe-carbonyl moiety, confirming that co-ordinated thiolates were able to capture Fe fragments with a degree of control over stoichiometry. Oxidation of [Ni(L)Fe(CO)$_4$] forms [Ni(L)Fe(CO)$_2$(L)Ni](BF$_4$)$_2$ (Fig. 14) in which Fe(0) has been oxidised to Fe(II) [79]. In [Ni(L)Fe(CO)$_2$(L)Ni]$^{2+}$ the Fe(II) ion is bridged to two Ni(L) units each through two thiolates bridges. The pseudo-octahedral geometry at Fe(II) is completed by the terminal co-ordination of two molecules of CO which are mutually *cis*, while the Ni remains in the Ni(II) formal oxidation state in a square-planar N_2S_2 donor set. On oxidation of [Ni(L)Fe(CO)$_4$] to [Ni(L)Fe(CO)$_2$(L)Ni](BF$_4$)$_2$ the Ni–S distances do not change significantly but the Ni–Fe distance decreases from 3.76(1) Å in [Ni(L)Fe(CO)$_4$] to 3.088 Å in

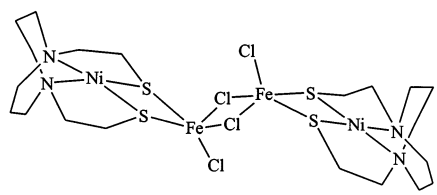

Fig. 12. The structure of [Ni(L)FeCl(μ-Cl_2)ClFe(L)Cl] [80].

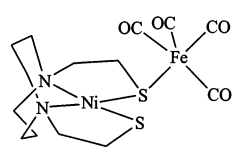

Fig. 13. The structure of [Ni(L)Fe(CO)$_4$] [79].

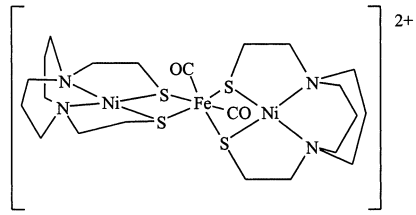

Fig. 14. The structure of $[Ni(L)Fe(CO)_2(L)\ Ni]^{2+}$ [79].

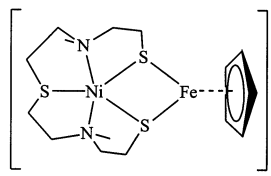

Fig. 15. The structure of $[Ni(L)FeCp]^+$ [81].

$[Ni(L)Fe(CO)_2(L)Ni](BF_4)_2$, and is accompanied by a decrease in the ∠Ni–S–Fe angle from 89.3(4) to 76.99(7) °.

Schröder and co-workers have recently obtained two structures incorporating dithiolate bridged Ni–Fe centres with short Ni–Fe distances related to the reduced form of the enzyme [81]. Reaction of (H_2L) [L = *N*,*N*′-dimethyl-*N*,*N*′-bis(2-mercaptoethyl)-bis(aminoethyl)sulphide] with Ni(II) forms [Ni(L)]. This Ni(II) thiolate complex was treated with $[FeCp(CO)_2I]$ to give [Ni(L)FeCp]I (Fig. 15), in which the Ni(II) ion is in a distorted square-pyramidal co-ordination geometry with the thioether donor at the apical position. Interestingly, the Ni–S(thioether) bond length is shorter than the Ni–S(thiolate bridge) distances: Ni–S(thioether) = 2.283(6) Å; Ni–S(thiolate bridge) 2.308(6): and 2.315(6) Å. The $Ni(\mu\text{-}S)_2Fe$ unit is V-shaped with a very acute ∠Ni–S–Fe bridging angle of 58–59 ° compared with 74 ° in [NiFe] hydrogenase from *D. gigas* [1,23]. A very acute ∠Ni–S–Fe angle brings the two metals within close proximity; Ni–Fe in $[Ni(L)FeCp]^+$ is 2.54 Å similar to the value of Ni–Fe distance observed in the Ni-SI form (2.5–2.6 Å) [22].

[Ni(L)FeCp]I can be metathesised to the PF_6^- salt $[Ni(L)FeCp]PF_6$ by addition of NH_4PF_6. $[Ni(L)FeCp]PF_6$ exhibits a quasi-reversible one-electron reduction at $E_{1/2} = -1.19$ V (vs. Fc/Fc^+) assigned to the Ni(II)/Ni(I) couple [81].

Recently Schröder and co-workers have investigated the possibility of preparing Ni–Fe complexes from a mononuclear Ni(II) thiolate precursor without the use of such highly chelating ligands, which have two major disadvantages. First, the chelating ligand has a preferred conformation and, in part, this dictates the stereochemistry around the ligated metal centre. Stereochemical rigidity also has an effect on the preferred oxidation states of the metal centres and often dictates the geometry of the Ni–Fe aggregate by preorganizing the direction of the sulphur orbitals. Secondly, chelating ligands involve donors with a very different bonding character to those found in the enzyme active site, most notably the use of

N-donors to model a Ni site ligated by soft sulphur donors. In order to reduce the rigidity of the system but maintain some control over the chemistry, a chelating phosphine ligand has been utilised to prepare mononuclear Ni(II) thiolate precursors. As the phosphine is a soft-donor, it is a better model for the cysteine sulphurs of the enzyme than the N-donors employed in other models. Thus, addition of $[Fe_3(CO)_{12}]$ to [(dppe)Ni(pdt)] (dppe = ethane-1,2-diphenylphosphine, pdt = 1,3-propanedithiolate) [82] in CH_2Cl_2 gives the neutral heterobimetallic complex $[(dppe)Ni(pdt)Fe(CO)_3]$ (Fig. 16) [81]. The use of the iron carbonyl precursor can be attributed to its lability but it may also be due to its covalent nature, and in this respect $Fe(CO)_3$ may be likened to the successful Fe synthon $Fe(NO)_2$. It should be noted that a bridging derivative of 1,3-propanedithiolate has been observed at the active site of [Fe]-only hydrogenase [6,7].

Comparison of Figs. 2 and 16 suggests that the structure of $[(dppe)Ni(pdt)Fe(CO)_3$ shows remarkable similarities to that of the active site of [NiFe] hydrogenase [1,23]. The Ni(II) and Fe(0) centres in $[(dppe)Ni(pdt)Fe(CO)_3]$ are only 2.466(6) Å apart consistent with a reduced form of the enzyme as measured by Maroney and co-workers for *C. vinosum* (Ni–Fe for Ni-SI is 2.5–2.6 Å) [22]. Ni(II) is in a distorted tetrahedral arrangement with the S1–S2–Ni and P1–P2–Ni planes twisted at an angle of 89 ° relative to one another, consistent with the arrangement of the cysteinate sulphurs observed in [NiFe] hydrogenase from *D. gigas* [1,23]. Notably, this is in contrast to the crystal structure of the precursor compound [(dppe)Ni(pdt)] which shows a square-planar P_2S_2 donor set at Ni(II) [81]. Thus, addition of the $Fe(CO)_3$ leads to a change in stereochemistry at Ni(II) from square-planar to tetrahedral. The presence of the 3- and 2-carbon linkers in the thiolates and phosphorus ligands, respectively, leads to ∠S–Ni–S and ∠P–Ni–P angles that are more acute (90 °) than the normal tetrahedral angle; this geometry is also observed for [NiFe] hydrogenase in *D. gigas* with a ∠S–Ni–S of 89 ° [1,23,52]. Indeed, recent work by Cramer and co-workers has focussed upon the potential spin state changes at the Ni(II) site in the reduced enzyme brought about by stereochemical distortion and/or addition of further ligands to give 5- or 6-coordinate species [22c].

The co-ordination geometry at Fe(0) in $[(dppe)Ni(pdt)Fe(CO)_3]$ is square-based pyramidal, with two CO ligands and two thiolate donors forming an almost perfect plane, and the third CO lying in an apical position. If the oxo bridging ligand is removed from the oxidised form of the enzyme (as expected for the more reduced forms) the geometry at Fe in $[(dppe)Ni(pdt)Fe(CO)_3]$ is remarkably similar in the enzyme and model consisting of three diatomics and two bridging thiolates [1,23].

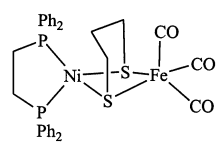

Fig. 16. The structure of $[(dppe)Ni(pdt)Fe(CO)_3]$ [81].

The thiolate ligand forms a chair at Fe and a boat at Ni, with an angle between the Ni–S1–S2 and Fe–S1–S2 planes of 80.3 ° compared with an angle of 81 ° in the enzyme [1,23,52].

3.1.2. Iron thiolate precursors

The second methodology that has been employed successfully to construct thiolate-bridged Ni–Fe cores is the application of a chelating thiolate ligand at Fe, and the reaction of this with a source of Ni(II).

A fascinating set of four redox-related complexes $[Fe(L)Ni(L)Fe]^{+/2+/3+/4+}$ [L^{3-} = 1,4,7-tris(4-*tert*-butyl-2-mercaptobenzyl)-1,4,7-triazacyclononane] was prepared by Wieghardt and co-workers [83–85] using this approach (Fig. 17). Reaction of the mononuclear species [Fe(L)] [85] with $NiCl_2 \cdot 6H_2O$ and subsequent metathesis yields $[Fe(L)Ni(L)Fe](PF_6)_2$, the crystal structure of which confirms the three face-sharing thiolate bridged octahedra with two terminal Fe(III) ions and a central Ni(II) ion (Fig. 17). The Ni–Fe distance of 3.054(1) Å is similar to that of 2.9 Å observed in oxidised *D. gigas* [1,23] and the Ni–S and Fe–S distances are between 2.345(1)–2.359(1) and 2.243(1)–2.248(1) Å, respectively, while the ∠Ni–S–Fe angles lie in the 83.02(4)–83.38(4) ° range. $[Fe(L)Ni(L)Fe](PF_6)_2$ exhibits three reversible redox processes, two reversible oxidations and a reversible reduction at $E_{1/2} = +0.69, -0.02$ and -0.90 V (vs. Fc/Fc^+) assigned to

$$[Fe(L)Ni(L)Fe]^{4+} \leftrightarrow [Fe(L)Ni(L)Fe]^{3+} \leftrightarrow [Fe(L)Ni(L)Fe]^{2+} \leftrightarrow [Fe(L)Ni(L)Fe]^{+}$$

Wieghardt concluded [85] that any assignment of the formal metal oxidation states to individual centres via a localised charge model was inappropriate as the one-electron oxidations and reductions affected all the three metal ions simultaneously. However, it was confirmed that the Fe ions remained equivalent in all four compounds. This is consistent with the computational studies of

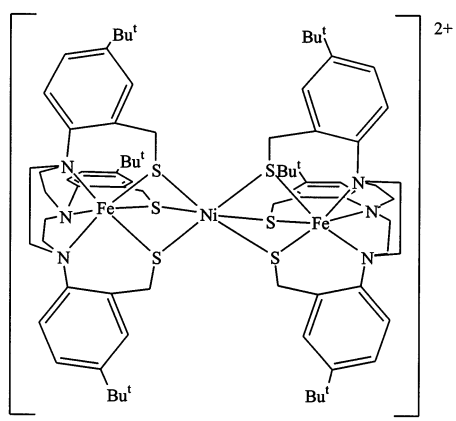

Fig. 17. The structure of $[Fe(L)Ni(L)Fe]^{2+}$ [83–85,85].

[NiFe] hydrogenase from *D. gigas* carried out by Gioia et al. [61] and Fontecilla-Camps and co-workers [62], who concluded that the redox chemistry of the active site involved the cluster as a whole, but that the Fe remained in the same redox state throughout.

Evans and co-workers have reported [86] the complex [{Fe(L)$(CO)_2$-*S*,*S*′}NiCl(dppe)] [$L^{3-} = N(CH_2CH_2S)_3^{3-}$] which incorporates a bis-thiolate bridged Ni–Fe centre (Fig. 18). This complex was prepared by the reaction of $[Fe(L)(CO)]^-$ with [dppe$NiCl_2$] under CO, and shows Ni(II) in a distorted square-pyramidal geometry with two bridging thiolate moieties occupying two *cis* positions in the basal plane. The remainder of the co-ordination sphere comprises a dppe molecule in the basal plane and a Cl^- ion at the axial position. The co-ordination geometry at Fe(II) in [{Fe(L)$(CO)_2$-*S*,*S*′}NiCl(dppe)] is distorted octahedral with the three thiolate donors arranged meridionally and the two bridging thiolates mutually *cis*. Co-ordination at Fe(II) is completed by the tertiary amine donor of L and two molecules of CO, the latter giving rise to two IR active stretches at 1944 and 2000 cm^{-1}. The feature at 1944 cm^{-1} is close to the observed value for the inactive oxidised form (Ni–A) form from *D. gigas* of 1947 cm^{-1} [18,19,28]. Although the Ni–Fe distance of 3.308(2) Å in [{Fe(L)$(CO)_2$-*S*,*S*′}NiCl(dppe)] is longer than those observed in complexes by Darensbourg and co-workers [80], Osterloh and co-workers [77,74] and Schröder and co-workers [81], this was the first literature example of a model complex that incorporates a bis-thiolate bridged heterodinuclear Ni–Fe centre and co-ordination of CO moieties at the Fe(II) centre [86].

3.2. Other methods

Recently, new methodologies for the preparation of Ni–Fe complexes have appeared in the literature, and these are reviewed in this section.

Kersting and co-workers have reported a Ni–Fe complex $[Fe^{III}(L)Ni^{II}]^{2+}$ with a bridging mixed amine thiophenolate ligand as shown in Fig. 19 [87]. The synthesis was achieved by addition of $NiCl_2$ followed by $FeCl_2$ to a solution of the ligand. The synthesis does not formally involve the formation of the Ni(II) complex as a direct precursor, but presumably this occurs *in situ*. In $[Fe^{III}(L)Ni^{II}]^{2+}$ both metals adopt an approximate octahedral co-ordination geometry consisting of three terminal amines and three bridging thiolate donors with a Ni–Fe distance of 3.030 Å. The complex $[Fe^{III}(L)Ni^{II}]^{2+}$, like the related model reported by Wieghardt and co-workers (Section 3.1.2) [83–85], has interesting electrochemical properties, and exhibits a reversible oxidation at $E_{1/2} = +0.45$ V and a reversible reduction at $E_{1/2} = -0.43$ vs. SCE. These redox states were characterised as:

$$[Ni^{III}(L)Fe^{III}]^{3+} \leftrightarrow [Ni^{II}(L)Fe^{III}]^{2+} \leftrightarrow [Ni^{II}(L)Fe^{II}]^{+}$$

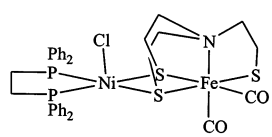

Fig. 18. The structure of [{Fe(L)$(CO)_2$-*S*,*S*′}NiCl(dppe)] [86].

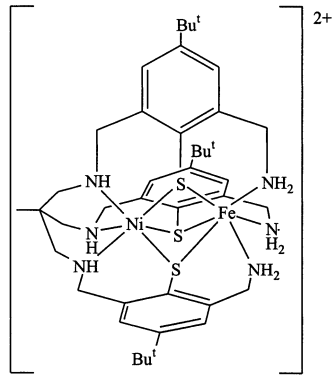

Fig. 19. The Structure of $[Fe(L)Ni]^{2+}$ [87].

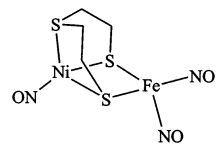

Fig. 20. The structure of $[(NO)Ni(\mu\text{-}SCH_2CH_2SCH_2CH_2S)Fe(NO)_2]$ [88].

The latest model published by Liaw et al. [88] is based on a methodology for the construction of Ni–Fe complexes from binuclear Ni(II) precursors. Thus, treatment of $[Ni(\mu\text{-}SCH_2CH_2SCH_2CH_2S)]_2$ with $[Fe(NO)_2(SePh)_2]^-$ in the presence of $NaNO_2$ yields $[(NO)Ni(\mu\text{-}SCH_2CH_2SCH_2CH_2S)Fe(NO)_2]$ (Fig. 20). This synthesis illustrates that a monometallic metal fragment with terminal thiolates is not a prerequisite for forming [NiFe] complexes, although mononuclear fragments may well be generated in solution. In $[(NO)Ni(\mu\text{-}SCH_2CH_2SCH_2CH_2S)Fe(NO)_2]$ the Ni(0) centre is in a distorted tetrahedral arrangement with S(thioether)–Ni–S(thiolate) angles of ca. 90 °. The ∠Fe–S–Ni angle is acute (75 °) giving a Ni–Fe distance of 2.8 Å, a very good fit to the central core of the oxidised form of the active site of [NiFe] hydrogenase from *D. gigas* (Ni–Fe 2.9 Å) [1,23]. $[(NO)Ni(\mu\text{-}SCH_2CH_2SCH_2CH_2S)Fe(NO)_2]$ exhibits an EPR spectrum with a single isotropic signal at $g = 2.021$. The complex shows two quasi-reversible processes at $E_{1/2} = +690$ mV and -970 mV (vs. NHE). Assuming that the $Fe(NO)_2$ group behaves as a covalently bonded moiety, the authors assigned the reduction process to:

$$Ni^0[Fe(NO)_2]^+ \leftrightarrow Ni^0[Fe(NO)_2]$$

The oxidation process was not assigned, the oxidised species being found to be EPR-silent.

4. Concluding remarks

A range of structures now mimic various aspects of the heterobinuclear Ni–Fe site in [NiFe] hydrogenase. Mono- di- and tri-thiolate-bridged heterodinuclear

Ni–Fe metal complexes have been prepared and characterised with Fe and Ni centres in 0 and +2 oxidation states. The terminal diatomics on Fe, the V-shaped geometry of the Ni(μ-S)$_2$Fe unit, the metal–metal separation, the stereochemistries at Ni and Fe, and the redox chemistry have been modelled to lesser or greater degrees. Many challenges remain for synthesis; the preparation of the heterometallic core in the presence of terminal thiolate donors on the same Ni presents a further important target, while models that reproduce the very narrow range of redox potentials of the enzyme and its reactivity towards H_2 will surely be developed in due course. We are beginning to understand the structure-reactivity relationships of thiolate complexes in the context of activity of [NiFe] hydrogenase activity. However, the many diverse and sometimes contradictory aspects of the active site need to converge into a functional low molecular weight model that will rationalise and lead to a better understanding *at the molecular level* of the factors that control and enable the function and activity of the metalloenzyme.

Note added in proof

For recent commentaries on [NiFe] hydrogenase reaction mechanisms, see M.J. Maroney, PA. Bryngelson, J. Biol. Inorg. Chem., 6 (2001) 453; P.E.M. Siegbahn, M.R.A. Blomberg, M. Wirstam née Pavlov, R.H. Crabtree, J. Biol. Inorg. Chem., 6 (2001) 460; H.-J. Fan, M.B. Hall, J. Biol. Inorg. Chem., 6 (2001) 467.

References

[1] A. Volbeda, M.-H. Charon, C. Piras, E.C. Hatchikian, M. Frey, J.C. Fontecilla-Camps, Nature 373 (1995) 580.
[2] T. Kentemich, G. Haverkamp, H. Bothe, Naturwissenschaften 77 (1990) 12.
[3] Y. Montet, E. Garcin, A. Volbeda, E.C. Hatchikian, M. Frey, J.C. Fontecilla-Camps, Pure Appl. Chem. 70 (1998) 25.
[4] M.C. Goldman, P.K. Mascharak, Comments Inorg. Chem. 18 (1995) 1.
[5] J.P. Collman, Nat. Struct. Biol. 3 (1996) 213.
[6] Y. Nicolet, C. Piras, P. Legrand, C.E. Hatchikian, J.C. Fontecilla-Camps, Structure 7 (1999) 13.
[7] J.W. Peters, W.N. Lanzilotta, B.J. Lemon, L.C. Seefeldt, Science 282 (1998) 1853.
[8] A.J. Pierek, M. Hulstein, W.R. Hagen, S.P.J. Albracht, Eur. J. Biochem. 258 (1998) 572.
[9] C. Zimgibl, W. van Dorgen, B. Schwörer, R. von Bünau, M. Richter, A. Klein, R.K. Thauer, Eur. J. Biochem. 208 (1992) 511.
[10] J.C. Fontecilla-Camps, S.W. Ragsdale, Adv. Inorg. Chem. 47 (1999) 283 (and references therein).
[11] M.K. Eidsness, R.A. Scott, B.C. Prickril, D.V. Dervartanian, J. Legall, I. Moura, J.J.G. Moura, H.D. Peck, Proc. Natl. Acad. Sci. USA 86 (1989) 197.
[12] W.-F. Liaw, Y.-C. Horng, D.-S. Ou, C.-Y. Ching, G.-H. Lee, S.-M. Peng, J. Am. Chem. Soc. 119 (1997) 9299.
[13] D.S. Patil, Methods Enzymol. 243 (1994) 68.
[14] E. Garcin, A. Volbeda, X. Vernade, E.C. Hatchikian, M. Frey, J.C. Fontecilla-Camps, Vth International Conference on Molecular Biology of Hydrogenases, Albertville, 1997, p. 37.
[15] Y. Montet, A. Volbeda, X. Vernede, M. Rousset, E.C. Hatchikian, M. Frey, J.C. Fontecilla-Camps, Vth International Conference on Molecular Biology of Hydrogenases, Albertville, 1997, p. 37.
[16] M. Texeira, G. Fauque, I. Moura, P.A. L'espinat, Y. Berlier, B. Prickrill Jr., H.D.P. Xavier, A.V. Legall, J.J.G. Moura, Eur. J. Biochem. 167 (1987) 47.

[17] R. Cammack, V.M. Fernandez, E.C. Hatchikian, in: H.D. Peck Jr., S. Legall (Eds.), Methods in Enzymology, vol. 243, Academic Press, San Diego, London, 1997, p. 43.
[18] R.P. Happe, W. Roseboom, A.J. Pierik, S.P.J. Albracht, K.A. Bagley, Nature 385 (1997) 126.
[19] K.A. Bagley, C.J.V. Gurderen, M. Chen, E.C. Duin, S.P.J. Albracht, W.H. Woodruff, Biochemistry 33 (1994) 9229.
[20] Ch. Gessner, M. Stein, S.P.J. Albracht, W. Lubitz, J. Biol. Inorg. Chem. 4 (1999) 379.
[21] O. Trofanchuk, M. Stein, Ch. Gessner, F. Lendzian, Y. Higuchi, W. Lubitz, J. Biol. Inorg. Chem. 5 (2000) 36.
[22] (a) G. Davidson, S.B. Choudhury, Z. Gu, K. Bose, W. Roseboom, S.P.J. Albracht, M.J. Maroney, Biochemistry 39 (2000) 7468;
(b) see also: E. Garcin, X. Vernede, E.C. Hatchikan, A. Volbeda, M. Frey, J.C. Fontecilla-Camps, Struct. Folding Des. 5 (1999) 557;
(c) H. Wang, C.Y. Ralston, D.S. Patil, R.M. Jones, W. Gu, M. Verhagen, M. Adams, P. Ge, C. Riordan, C.A. Marganian, P. Mascharak, J. Kovacs, C.G. Miller, T.J. Collins, S. Brooker, P.D. Croucher, K. Wang, E.I. Stiefel, S.P. Cramer, J. Am. Chem. Soc. 122 (2000) 10544 and references therein.
[23] A. Volbeda, E. Garain, C. Piras, A.L. Delacey, V.M. Fernandez, E.C. Hatchikian, M. Frey, J.C. Fontecilla-Camps, J. Am. Chem. Soc. 118 (1996) 12989.
[24] E.C. Hatchikian, M. Bruschi, J. LeGall, Biochem. Biophys. Res. Commun. 82 (1978) 451.
[25] R. Cammack, D. Patil, R. Aguire, E.C. Hatchikian, FEBS Lett. 142 (1982) 289.
[26] J. LeGall, P.O. Ljungdahl, I. Moura, H.D. Peck, A. Xavier, J.J.G. Moura, M. Tiexeira, B.H. Huyn, D.V. DerVartanian, Biochem. Biophys. Res. Commun. 106 (1982) 610.
[27] M. Frey, Struct. Bonding 90 (1998) 98 (and references therein). Since submission of the manuscript a review has appeared; M.Y. Darensbourg, E.J. Lyon and J.J. Smee, Coord. Chem. Rev., 206–207 (2000) 533.
[28] A.L. Delacey, E.C. Hatchikian, A. Volbeda, M. Frey, J.C. Fontecilla-Camps, V.M. Fernandez, J. Am. Chem. Soc. 119 (1997) 7181.
[29] Y. Higuchi, T. Yagi, N. Yasuoka, Structure 5 (1997) 1671.
[30] M.A. Halcrow, G. Christou, Chem. Rev. 94 (1994) 2421.
[31] J.C. Fontecilla-Camps, Struct. Bonding 91 (1998) 1.
[32] D.P. Barondeau, L.M. Roberts, P.A. Lindahl, J. Am. Chem. Soc. 116 (1994) 3442.
[33] M. Kumar, R.O. Day, G.J. Colpas, M.J. Maroney, J. Am. Chem. Soc. 111 (1989) 5974.
[34] C.A. Grapperhaus, M.Y. Darensbourg, Acc. Chem. Res. 31 (1998) 451.
[35] R. Cammack, D. Patil, R. Aguirre, E.C. Hatchikian, FEBS Lett. 142 (1982) 289.
[36] V.M. Fernandez, R. Aguirre, E.C. Hatchikian, Biochim. Biophys. Acta 790 (1984) 1.
[37] V.M. Fernandez, E.C. Hatchikian, R. Cammack, Biochem. Biophys. Acta 832 (1985) 69.
[38] J.W. van der Swaan, S.P.J. Albracht, R.D. Fontjin, S.C. Slater, FEBS Lett. 179 (1985) 271.
[39] V.M. Fernandez, E.C. Hatchikian, D.S. Patil, R. Cammack, Biochem. Biophys. Acta 883 (1986) 145.
[40] M. Medina, E.C. Hatchikian, R. Cammack, Biochem. Biophys. Acta 1275 (1996) 227.
[41] J.R. Lancaster (Ed.), Bioinorganic Chemistry of Nickel, VCH, Weinheim, 1988 (and references therein).
[42] D.P. Barondeau, L.M. Roberts, P.A. Lindahl, J. Am. Chem. Soc. 116 (1994) 3442.
[43] J.M.C.C. Coremans, C.J. van Garderen, S.P.J. Albracht, Biochim. Biophys. Acta 1119 (1992) 148.
[44] S.P.J. Albracht, Biochim. Biophys. Acta 1188 (1994) 167.
[45] L.M. Roberts, P.A. Lindahl, Biochemistry 33 (1994) 14339.
[46] R. Cammack, D.S. Patil, E.C. Hatchikan, V.M. Fernandez, Biochim. Biophys. Acta 912 (1987) 98.
[47] N. Baidya, M. Olmstead, P.K. Mascharak, Inorg. Chem. 30 (1991) 929.
[48] N. Baidya, M. Olmstead, J.P. Whitehead, C. Bagyinka, M.J. Maroney, P.K. Mascharak, Inorg. Chem. 31 (1992) 3612.
[49] N. Baidya, M. Olmstead, P.K. Mascharak, J. Am. Chem. Soc. 114 (1992) 9666.
[50] P.J. Farmer, J.H. Reibenspies, P.A. Lindahl, M.Y. Darensbourg, J. Am. Chem. Soc. 115 (1993) 4665.
[51] F. Dole, A. Fournel, V. Magro, E.C. Hatchikian, P. Bertrand, B. Guigliarelli, Biochemistry 36 (1997) 7847.
[52] J.C. Fontecilla-Camps, J. Biol. Inorg. Chem. 91 (1996) 1 (and references therein).
[53] J.C. Fontecilla-Camps, A. Volbeda, M. Frey, TIBTECH 14 (1997) 417.
[54] D. Sellmann, F. Geipel, M. Moll, Angew. Chem. Int. Ed. Engl. 39 (2000) 561.

[55] D. Sellmann, G.H. Rackelmann, F.W. Heinemann, Chem. Eur. J. 3 (1997) 2071.
[56] S.C. Shoner, M.M. Olmstead, J.A. Kovacs, Inorg. Chem. 33 (1994) 7 (and references therein).
[57] L.M. Roberts, P.A. Lindahl, J. Am. Chem. Soc. 117 (1995) 2565.
[58] M. Teixeira, I. Moura, A.V. Xavier, J.J.G. Moura, J. LeGall, D.V. DerVartanian, H.D. Peck Jr, B.H. Huynh, J. Biol. Chem. 264 (1989) 16435.
[59] R. Cammack, D. Patil, E.C. Hatchikian, V.M. Fernandez, Biochim. Biophys. Acta 912 (1987) 98.
[60] M. Teixeira, I. Moura, A.V. Xavier, J.J.G. Moura, J. LeGall, D.V. DerVartanian, H.D. Peck Jr, B.H. Huynh, Eur. J. Biochem. 130 (1983) 481.
[61] L.de. Gioia, P. Fantuca, B. Guigliarelli, P. Bertrand, Inorg. Chem. 38 (1999) 2658.
[62] P. Amara, A. Volbeda, J.C. Fontecilla-Camps, M.J. Field, J. Am. Chem. Soc. 121 (1999) 4468.
[63] S. Niu, L.M. Thomson, M.B. Hall, J. Am. Chem. Soc. 121 (1999) 4000.
[64] (a) H.-J. Krüger, R.H. Holm, J. Am. Chem. Soc. 26 (1987) 3645;
(b) H.-J. Krüger, R.H. Holm, Inorg. Chem. 28 (1989) 1148;
(c) H.-J. Krüger, R.H. Holm, J. Am. Chem. Soc. 112 (1990) 2955;
(d) H.-J. Krüger, G. Peng, R.H. Holm, Inorg. Chem. 30 (1991) 734.
[65] (a) A.J. Atkins, A.J. Blake, M. Schröder, J. Chem. Soc. Chem. Commun. (1993) 1662;
(b) A.J. Atkins, A.J. Blake, D. Black, A. Marin-Becerra, S. Parsons, L. Ruiz-Ramirez, M. Schröder, J. Chem. Soc. Chem. Commun. (1996) 457;
(c) N.D.J. Branscombe, A.J. Blake, A. Marin-Becerra, W.-S. Li, S. Parsons, L. Ruiz-Ramirez, M. Schröder, J. Chem. Soc. Chem. Commun. (1996) 2573.
[66] (a) A.J. Blake, R.O. Gould, M.A. Halcrow, A.J. Holder, M. Schröder, J. Chem. Soc. Dalton Trans. (1992) 3427;
(b) A.J. Blake, R.O. Gould, M.A. Halcrow, M. Schröder, J. Chem. Soc. Dalton Trans. (1993) 2909.
[67] S. Brooker, G.B. Caygill, P.D. Croucher, T.C. Davidson, D.L.J. Clive, S.R. Magnuson, S.P. Cramer, C.Y. Ralston, J. Chem. Soc. Dalton Trans. (2000) 3113 (and references therein).
[68] J. Hanss, H.-J. Krüger, Angew. Chem. Int. Ed. Engl. 37 (1998) 360.
[69] G.B. Allan, G. Davidson, S.B. Choudhury, Z. Gu, K. Bose, R.O. Day, G. Davidson, M.J. Maroney, Inorg. Chem. 37 (1998) 4166.
[70] G.J. Colpas, M. Kumar, R.O. Day, M.J. Maroney, Inorg. Chem. 29 (1990) 4779.
[71] G.J. Colpas, R.O. Day, M.J. Maroney, Inorg. Chem. 31 (1992) 5053.
[72] T.B. Rauchfuss, D.M. Roundhill, J. Am. Chem. Soc. 97 (1975) 3386.
[73] E. Bouwmann, R.K. Henderson, A.L. Spek, J. Reedijk, Eur. J. Inorg. Chem. (1999) 217.
[74] F. Osterloh, W. Saak, D. Haase, S. Pohl, J. Chem. Soc. Chem. Commun. (1996) 777.
[75] H. Okuno, K. Uoto, O. Yonemitsu, T. Tomohiro, J. Chem. Soc. Chem. Commun. (1987) 1018.
[76] W. Saak, S. Pohl, Z. Naturforsch. Teil B 40 (1985) 1105.
[77] F. Osterloh, W. Saak, D. Haase, S. Pohl, J. Chem. Soc. Chem. Commun. (1997) 979.
[78] D.K. Mills, Y.M. Hsiao, P.J. Farmer, E.V. Atnip, J.H. Reibenspies, M.Y. Darensbourg, J. Am. Chem. Soc. 113 (1991) 1421.
[79] C.H. Lai, J.H. Reibenspies, M.Y. Darensbourg, Angew. Chem. Int. Ed. Engl. 35 (1996) 2390.
[80] D.K. Mills, J.H. Reibenspies, M.Y. Darensbourg, Inorg. Chem. 29 (1990) 4364.
[81] (a) D.J.E. Spencer, A.J. Blake, P.A. Cooke, M. Schröder, J. Inorg. Biochem. 74 (1999) 303;
(b) A.J. Blake, P.A. Cooke, A.C. Marr, D.J.E. Spencer, C. Wilson, M. Schröder, submitted for publication.
[82] M. Schmidt, G.G. Hoffmann, J. Organomet. Chem. 124 (1977) C5.
[83] T. Glaser, F. Kersting, T. Beissel, E. Bill, T. Weyhermüller, W. Meyer-Klaucke, K. Wieghardt, Inorg. Chem. 38 (1999) 722.
[84] T. Glaser, T. Beissel, E. Bill, T. Weyhermüller, V. Schünemann, W. Meyer-Klaucke, A.X. Trautwein, K. Wieghardt, J. Am. Chem. Soc. 121 (1999) 2193.
[85] T. Beissel, K.S. Bürger, G. Voigt, K. Wieghardt, C. Butzlaff, A.X. Trautwein, Inorg. Chem. 32 (1993) 124.
[86] S.C. Davies, D.J. Evans, D.L. Hughes, S. Longhurst, J.R. Sanders, J. Chem. Soc. Chem. Commun. (1999) 1935; see also M.C. Smith, S. Longhurst, J.E. Barclay, S.P. Gamer, S.C. Davies, D.L. Hughes, W.-W. Gu, D.J. Evans, J. Chem. Soc., Dalton Trans. (2001) 1387.
[87] G. Steinfeld, B. Kersting, Chem. Commun. (2000) 205.
[88] W.F. Liaw, C.Y. Chiang, G.H. Lee, S.M. Peng, C.H. Lai, M.Y. Darensbourg, Inorg. Chem. 39 (2000) 480.